

# Memristor mathematical model, ver. 1.0

<https://github.com/eugnsp/memristor>

January 12, 2019

## Contents

<b>1</b>	<b>Introduction</b>	<b>1</b>
<b>2</b>	<b>Heat equation</b>	<b>2</b>
2.1	Boundary conditions . . . . .	3
2.2	Discretization . . . . .	3
<b>3</b>	<b>Poisson's equation</b>	<b>4</b>
3.1	Boundary conditions . . . . .	5
3.2	Discretization . . . . .	5
<b>4</b>	<b>Kinetic Monte-Carlo method</b>	<b>5</b>
4.1	Initial conditions . . . . .	6
4.2	Boundary conditions . . . . .	6
4.3	Algorithm . . . . .	6
<b>5</b>	<b>Core resistance, potential and heat source</b>	<b>7</b>
<b>6</b>	<b>Device simulation algorithm</b>	<b>8</b>

## 1 Introduction

This is a succinct formal description of equations, their discretization and algorithms used for memristor modelling. Gauss units are used in equations and atomic units are used in the code.

We assume the system to be cylindrically symmetric. 2D finite element schemes are employed for the Poisson and the heat equations. A 3D grid is used for the Monte-Carlo simulation of O-vacancies motion with subsequent averaging over the polar angle.

The geometry of the system is shown in fig. 1. The geometry is defined in an external mesh file. Numerical physical tags in the mesh file are used to discern different regions.

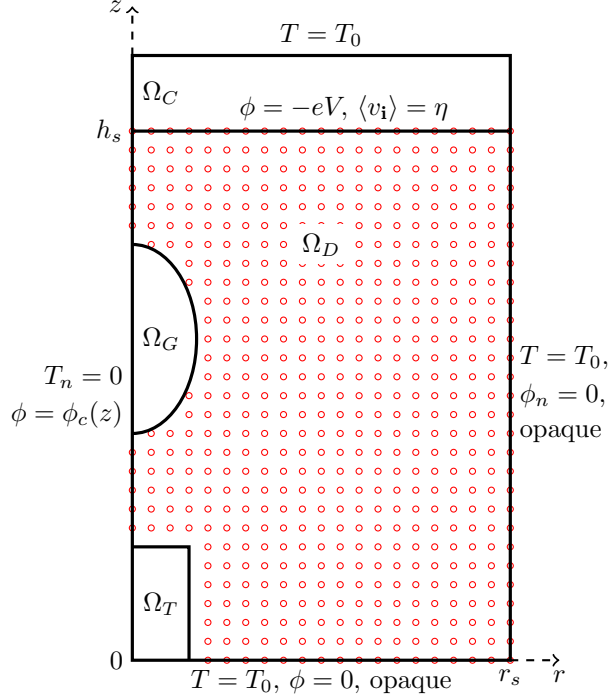


Figure 1: Geometry of the system ( $\Omega_T$  — metallic tip,  $\Omega_G$  — metallic granule(s),  $\Omega_C$  — top contact,  $\Omega_D$  — dielectric matrix), and boundary conditions. The projection of the Monte-Carlo 3D grid onto the ( $\phi = 0$ )-plane is shown with red circles.

## 2 Heat equation

The heat equation for the lattice temperature  $T(\mathbf{x})$  is

$$-\nabla \cdot [c(\mathbf{x})\nabla T(\mathbf{x})] = s(\mathbf{x}), \quad (1)$$

where  $c(\mathbf{x})$  is the thermal conductivity, and  $s(\mathbf{x})$  is the volume heat density of the source. The equation is solved in the whole area

$$\Omega_H = \Omega_D \cup \Omega_G \cup \Omega_T \cup \Omega_C. \quad (2)$$

In the cylindrical coordinates this equation for  $T(\mathbf{x}) = T(r, z)$  takes the form:

$$-\frac{\partial}{\partial r} \left[ c(r, z) \frac{\partial T}{\partial r} \right] - \frac{c(r, z)}{r} \frac{\partial T}{\partial r} - \frac{\partial}{\partial z} \left[ c(r, z) \frac{\partial T}{\partial z} \right] = s(r, z). \quad (3)$$

The structure of the heat source term is

$$s(r, z) = \frac{\theta[r_0(z) - r]}{\pi r_0(z)^2} s(z), \quad (4)$$

where  $r_0(z)$  is the source radius, and  $s(z)$  is its linear density. It is tempting to approximate the source with a delta-functional one

$$s(r, z) = \delta(\pi r^2) s(z) = \frac{\delta(r)}{2\pi r} s(z). \quad (5)$$

However, the solution of (3) is singular at  $r = 0$ :  $T(r) \sim \ln(r)$ . Hence, finite  $r_0$  should be retained. For simplicity we assume  $r_0 := \{\text{heat\_source\_radius}\}$  to be independent of  $z$ . Due to the logarithmic divergence the solution is very sensitive to the value of  $r_0$  for  $r < r_0$ .

The thermal conductivity is assumed to be uniform in the whole system:

$$c(r, z) = c := \{\text{thermal\_conductivity}\}. \quad (6)$$

## 2.1 Boundary conditions

The uniform Dirichlet boundary condition is assumed at the outer surface:

$$T(\mathbf{x})|_{\Gamma_1} = T_0 := \{\text{temperature}\}, \quad \Gamma_1 = \partial\Omega_H \setminus \{r = 0\}. \quad (7)$$

This condition translates into the following condition in the cylindrical coordinates:

$$T(r, z)|_{\Gamma_1} = T_0. \quad (8)$$

along with the compatibility condition at  $r = 0$

$$\left. \frac{\partial T(r, z)}{\partial r} \right|_{\Gamma_2} = 0, \quad \Gamma_2 = \partial\Omega_H \cap \{r = 0\}. \quad (9)$$

## 2.2 Discretization

Multiplying eq. (3) by  $r$ , we obtain

$$-r\nabla \cdot (c\nabla T) - c \frac{\partial T}{\partial r} = \frac{I^2}{\pi r_0^2} \theta(r_0 - r) r c, \quad \nabla = (\partial_r, \partial_z). \quad (10)$$

After multiplication by a test function  $\chi(r, z)$  and integration by parts we get

$$\begin{aligned} - \int_{\Omega_H} r \chi \nabla \cdot (c \nabla T) - \int_{\Omega_H} \chi c \frac{\partial T}{\partial r} &= \\ &= \int_{\Omega_H} c [\nabla(r\chi) \cdot \nabla T] - \int_{\partial\Omega_H} r \chi c (\nabla T \cdot \hat{\mathbf{n}}) - \int_{\Omega_H} \chi c \frac{\partial T}{\partial r} = \\ &= \int_{\Omega_H} r c (\nabla \chi \cdot \nabla T) - \int_{\partial\Omega_H} r \chi c (\nabla T \cdot \hat{\mathbf{n}}) = \frac{I^2}{\pi r_0^2} \int_{\Omega_H} r \chi \theta(r_0 - r) r c. \end{aligned} \quad (11)$$

The space of test functions is chosen such that  $\chi$  vanishes at the Diriclet boundary. Then due to the compatibility condition (9) the boundary term drops out:

$$\int_{\Omega_H} rc(\nabla\chi \cdot \nabla T) = \frac{I^2}{\pi r_0^2} \int_{\Omega_H} r\chi\theta(r_0 - r)r_c. \quad (12)$$

To account for non-zero Dirichlet boundary conditions, we make a substitution  $T \rightarrow T + T_b$ , where  $T$  now has zero boundary conditions, and  $T_b$  is an arbitrary function such that  $T_b|_{\Gamma} = T_0$ :

$$\int_{\Omega_H} rc(\nabla\chi \cdot \nabla T) = \frac{I^2}{\pi r_0^2} \int_{\Omega_H} r\chi\theta(r_0 - r)r_c - \int_{\Omega_H} rc(\nabla\chi \cdot \nabla T_b) \quad (13)$$

Expanding  $T = \sum_j T_j \chi_j$  over basis functions  $\chi_i$  and using the Galerkin's method, we get the discrete system for the  $T_j$  coefficients:

$$\sum_j S_{ij} T_j = b_i, \quad (14)$$

where

$$S_{ij} = \int_{\Omega_H} rc(\nabla\chi_i \cdot \nabla\chi_j), \quad b_i = \frac{I^2}{\pi r_0^2} \int_{\Omega_H} r\chi_i\theta(r_0 - r)r_c - \int_{\Omega_H} rc(\nabla\chi_i \cdot \nabla T_b). \quad (15)$$

### 3 Poisson's equation

The Poisson's (Laplace's) equation for the electrostatic potential  $\phi(\mathbf{x})$  with zero charge density is

$$\nabla[\epsilon(\mathbf{x})\nabla\phi(\mathbf{x})] = 0, \quad (16)$$

where  $\epsilon(\mathbf{x})$  is the dielectric permittivity.

The equation is solved in the area

$$\Omega_P = \Omega_D \cup \Omega_G \cup \Omega_T. \quad (17)$$

For  $\phi(\mathbf{x}) = \phi(r, z)$  this equation takes the form:

$$-\frac{\partial}{\partial r} \left( \epsilon \frac{\partial \phi}{\partial r} \right) - \frac{\epsilon}{r} \frac{\partial \phi}{\partial r} - \frac{\partial}{\partial z} \left( \epsilon \frac{\partial \phi}{\partial z} \right) = 0. \quad (18)$$

Due to the vanishing charge density the absolute value of  $\epsilon$  is not important. The following values are used:

$$\epsilon(\mathbf{x}) = \begin{cases} 1, & \mathbf{x} \in \Omega_D, \\ 100, & \mathbf{x} \in \Omega_T \cup \Omega_G, \end{cases} \quad (19)$$

where  $100 \gg 1$  is an arbitrary constant used to model a metallic region where the potential is constant.

### 3.1 Boundary conditions

Dirichlet boundary conditions are used at the contacts and along the core:

$$\phi(\mathbf{x})|_{\Gamma_3} = 0, \quad \Gamma_3 = \partial\Omega_P \cap \{z = 0\}, \quad (20)$$

$$\phi(\mathbf{x})|_{\Gamma_4} = V, \quad \Gamma_4 = \partial\Omega_P \cap \{z = h_s\}, \quad (21)$$

$$\phi(\mathbf{x})|_{\Gamma_5} = \phi_c(z), \quad \Gamma_5 = \partial\Omega_P \cap \{r = 0\}, \quad (22)$$

where  $V$  is the external bias voltage, and  $\phi_c(z)$  is the potential along the core.

At the outer boundary zero Neumann condition is used:

$$\left. \frac{\partial\phi}{\partial r} \right|_{\Gamma_6} = E_n = 0, \quad \Gamma_6 = \partial\Omega_P \cap \{r = r_s\}. \quad (23)$$

### 3.2 Discretization

The Poisson equation has the same type as the heat equation, and its discretization follows the same lines. The result is:

$$S_{ij} = \int_{\Omega_P} r(\nabla\chi_i \cdot \nabla\chi_j), \quad b_i = - \int_{\Omega_P} r(\nabla\chi_i \cdot \nabla\phi_b), \quad (24)$$

where  $\phi_b$  is an arbitrary function that satisfies non-zero Dirichlet boundary conditions.

## 4 Kinetic Monte-Carlo method

The distribution of vacancies is described by the occupation numbers  $v_{\mathbf{i}}$ , which can only be 0 (no vacancy) or 1 (single vacancy), with indices  $\mathbf{i}$  defined on the discrete 3D uniform grid  $\mathcal{G}$ ,

$$\mathcal{G} = \{\mathbf{i} = (i, j, k) \mid \mathbf{x}_{\mathbf{i}} \in \bar{\Omega}_D \setminus (\bar{\Omega}_T \cup \bar{\Omega}_G)\}, \quad (25)$$

where  $\mathbf{x}_{\mathbf{i}}$  are the coordinates of the site  $\mathbf{i}$ . The grid spacing equals  $\delta := \{\text{grid\_delta}\}$ .

It is assumed that vacancies hop only between nearest-neighbour sites. Each site (except for boundary ones) has six nearest neighbours. The rate (probability per unit time) of hopping is

$$\Gamma_{\mathbf{i} \rightarrow \mathbf{i}'} = v_{\mathbf{i}}(1 - v_{\mathbf{i}'})\Gamma'_{\mathbf{i} \rightarrow \mathbf{i}'}, \quad \Gamma'_{\mathbf{i} \rightarrow \mathbf{i}'} = w_0 \exp \left\{ - \frac{E_{ac} + q[\phi(\mathbf{x}_{\mathbf{i}'} - \phi(\mathbf{x}_{\mathbf{i}})]}{T[(\mathbf{x}_{\mathbf{i}} + \mathbf{x}_{\mathbf{i}'})/2]} \right\}, \quad (26)$$

where  $w_0 := \{\text{debye\_frequency}\}$  is the Debye frequency,  $T(\mathbf{x})$  is the temperature,  $\phi(\mathbf{x})$  is the electrostatic potential, and  $q = e > 0$  is the O-vacancy charge. The pre-factor  $v_{\mathbf{i}}(1 - v_{\mathbf{i}'})$  takes into account that the hopping is possible only if the source site is occupied ( $v_{\mathbf{i}} = 1$ ) and the destination one is empty ( $v_{\mathbf{i}'} = 0$ ).

## 4.1 Initial conditions

Initially all vacancies are distributed uniformly randomly over  $\mathcal{G}$  with the filling factor  $\eta := \{\text{initial\_filling}\}$ ,  $\eta \in (0, 1)$ , such that the total number of vacancies is  $\lfloor \eta N_{\mathcal{G}} \rfloor$ , where  $N_{\mathcal{G}}$  is the total number of sites in  $\mathcal{G}$ .

## 4.2 Boundary conditions

If the source or final site lies outside the domain  $\Omega_D$ , the hopping rates are determined by the boundary conditions. All boundaries, except for

$$\Gamma_M = \partial\Omega_D \cap \{z = h_s\}, \quad (27)$$

are impenetrable, i. e. corresponding rates for each boundary site  $\mathbf{i}$  vanish:

$$\Gamma_{\bullet \rightarrow \mathbf{i}} = 0, \quad \Gamma_{\mathbf{i} \rightarrow \bullet} = 0, \quad (28)$$

where  $\bullet$  denotes a “virtual” site outside the system.

If a site  $\mathbf{i}$  has the total in-scattering rate  $\Gamma_{\text{in}}$  and the total out-scattering rate  $\Gamma_{\text{out}}$ , then its time-averaged population at large time scale  $t \gg \Gamma_{\text{in}}^{-1} + \Gamma_{\text{out}}^{-1}$  is

$$\langle v_{\mathbf{i}} \rangle_t = \frac{\Gamma_{\text{out}}^{-1}}{\Gamma_{\text{in}}^{-1} + \Gamma_{\text{out}}^{-1}} = \frac{1}{1 + \Gamma_{\text{out}}/\Gamma_{\text{in}}}. \quad (29)$$

At  $\Gamma_M$  we require the time-averaged population to be equal to the initial filling factor  $\eta$ :  $\langle v_{\mathbf{i}} \rangle = \eta$ . Hence, if a boundary site  $\mathbf{i} \in \Gamma_M$  is empty, the in-scattering rate  $\Gamma_{\bullet \rightarrow \mathbf{i}}$  is

$$\Gamma_{\bullet \rightarrow \mathbf{i}} = \frac{\eta}{1 - \eta} \sum_{\mathbf{i}'} (1 - v_{\mathbf{i}'}) \Gamma'_{\mathbf{i} \rightarrow \mathbf{i}'}, \quad (30)$$

and if it is occupied, the out-scattering rate  $\Gamma_{\mathbf{i} \rightarrow \bullet}$  is

$$\Gamma_{\mathbf{i} \rightarrow \bullet} = \frac{1 - \eta}{\eta} \sum_{\mathbf{i}'} v_{\mathbf{i}'} \Gamma'_{\mathbf{i}' \rightarrow \mathbf{i}}. \quad (31)$$

## 4.3 Algorithm

Variable step size method is used for Monte-Carlo simulation. The following algorithm is used:

1. **Initialization.** Identify all possible events and compute their rates  $\{\Gamma_k = \Gamma_{\mathbf{i} \rightarrow \mathbf{i}'}, \Gamma_{\bullet \rightarrow \mathbf{i}}, \Gamma_{\mathbf{i} \rightarrow \bullet}\}$ .
2. **Main loop.** Compute probabilities of all events  $\{P_k = \Gamma_k/\Gamma\}$ , where  $\Gamma = \sum_k \Gamma_k$  is the total rate. Select the next event index  $n$  randomly according to this probability distribution: take a uniform random number  $v \in (0, 1)$  and find the smallest  $n$  such that  $\sum_k^n \Gamma_k \geq v\Gamma$ .

3. Update the list of possible events, calculate new  $\{\Gamma_k\}$ , and recalculate those old  $\{\Gamma_k\}$  that could have changed.
4. Compute the time step  $\Delta t_i = -\ln u/\Gamma$ , where  $u \in (0, 1)$  is a uniform random number (independent of  $v$ ).
5. Check if the total simulation duration  $\Delta t = \sum_i \Delta t_i$  and/or the number of steps exceed the given limits. Abort, if they do.
6. Go to step 2.

Fenwick tree data structure is used for fast determination of the next event index in the step 2 and event table updates in the step 3.

## 5 Core resistance, potential and heat source

If the core has linear resistivity  $r_c(z)$ , then the potential along the core and the linear heat density due to the Joule heating are:

$$\phi_c(z) = I \int_0^z dz' r_c(z'), \quad s(z) = I^2 r_c(z), \quad (32)$$

where  $I$  is the total current:

$$I = \frac{V}{R}, \quad R = \int_0^{h_s} dz r_c(z). \quad (33)$$

To compute the linear resistivity, we assume that the core is separated into sections of three types: (1) metallic tip and granule(s) with zero resistivity; (2) grain boundary with linear resistivity  $r_g := \{\text{grain\_bnd\_resistivity}\}$  independent of  $z$ , if no filament is formed at  $z$ ; (3) filament with linear resistivity

$$r_f(z) = \frac{\rho_0}{\pi R_f^2(z)}, \quad (34)$$

where  $\rho_0 := \{\text{filament\_resistivity}\}$  is the filament volume resistivity, and  $R_f(z)$  is its radius.

After discretization, the linear resistivity  $r_c(z)$  is represented by  $r_c(z_i)$  at the points  $z_i = i\delta$ . If  $z_i \in \overline{\Omega}_T \cup \overline{\Omega}_G$ , then  $r_c(z_i) = 0$ . Otherwise,  $r_c(z_i)$  depends on whether the filament is formed at  $z = z_i$  or not.

We assume that the filament has radial symmetry. Its shape is described by the filament radius function  $R_f(z)$ . It is defined as follows:

$$R(z_i) = \max_{\substack{r \geq r_{\min}, \\ N_f(r)/N(r) \geq \xi}} r, \quad (35)$$

where  $N_f(r)$  ( $N(r)$ ) is the number of filled (total) sites  $\{j\}$  in the grid  $\mathcal{G}$  that have coordinates  $(x_j^2 + y_j^2 \leq r^2, z_j = z_i)$ ,  $\xi := \{\text{filament\_filling\_threshold}\}$  is the

filling threshold, and  $r_{\min} > 0$  is the minimal filament radius. If no such max exists, it is assumed that no filament is formed at  $z = z_i$ .

Numerically, max in the definition above is sought for over a discrete set of radii  $\{n\delta \mid n \in \mathbb{Z}\}$  using simple linear search. Minimal radius is given by  $r_{\min} = n_{\min}\delta$  with  $n_{\min} := \{\text{min\_filament\_radius}\}$ .

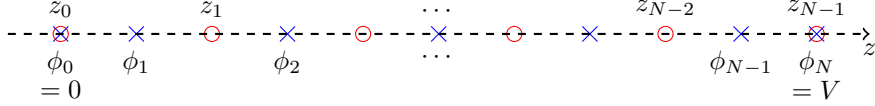


Figure 2: Discretization of the core potential  $\phi_i = \phi(z_{i-1/2})$ ;  $\phi_0$  and  $\phi_N$  are special and hold boundary conditions.

The discretized core potential is defined at  $z_0 = 0$ ,  $z_{N-1} = h_s$  and the mid-points  $z_{i+1/2} = (z_i + z_{i+1})/2$ , see fig. 2:

$$\begin{aligned}
\phi_0 &= 0, \\
\phi_1 &= \phi(z_{1/2}) = I \frac{r_c(z_0)\delta}{2}, \\
\phi_2 &= \phi(z_{3/2}) = I \left[ \frac{r_c(z_0)}{2} + r_c(z_1) \right] \delta, \\
&\dots \\
\phi_N &= \phi(z_{N-1}) = IR = V.
\end{aligned} \tag{36}$$

where the total resistance  $R$  is:

$$R = \left[ \frac{r_c(z_0)}{2} + r_c(z_1) + \dots + r_c(z_{N-2}) + \frac{r_c(z_{N-1})}{2} \right] \delta. \tag{37}$$

## 6 Device simulation algorithm

To limit the maximum current through the system, we introduce a non-linear limiting resistance  $R_{\text{lim}}(V)$  connected in series with the system, such that the total resistance is  $R_{\text{tot}} = R + R_{\text{lim}}$ . Its value is adjusted in a self-consistent manner:

$$R_{\text{lim}}(V) = \begin{cases} 0, & I_m R \geq V, \\ \frac{V}{I} - R, & I_m R < V, \end{cases} \tag{38}$$

where  $I_m$  is the maximum current, and  $V$  is the total bias voltage.

The device simulation proceeds according to the following algorithm:

1. **Initialization.** Read the mesh for the heat equations from the external file; create the mesh for the Poisson equation; initialize the finite-element solvers; initialize the Monte-Carlo solver; generate the initial distribution of O-vacancies.



2. Set bias voltage to zero:  $V \leftarrow 0$ ; set bias voltage sweep direction to “forward”:  $\xi \leftarrow +1$ .
3. **Main loop.** Compute the filament shape.
4. Compute the linear resistance  $r_c(z)$ ; compute the total current  $I$ ; compute the linear heat source density  $I^2 r_c(z)$ ; compute the Poisson equation boundary condition  $\phi(0, z)$ .
5. Solve the heat equation for  $T(r, z)$ ; solve the Poisson equation for  $\phi(r, z)$ ; interpolate to the Monte-Carlo grid to obtain  $T(\mathbf{x}_i)$  and  $\phi(\mathbf{x}_i)$ .
6. Estimate the duration  $\langle \Delta t \rangle$  of a single Monte-Carlo step. If it is larger than the minimum Monte-Carlo step duration  $\langle \Delta t \rangle_{\min} := \{\text{min\_step\_duration}\}$ , set time step:  $\Delta t \leftarrow \overline{\Delta t}_{\min}$ , and go to step 8 (skip Monte-Carlo simulation).
7. Run the Monte-Carlo simulation for  $n := \{\text{steps\_per\_round}\}$  steps; compute the elapsed time  $\Delta t$ .
8. Update bias voltage:  $V \leftarrow V + \xi s \Delta t$ , where  $s := \{\text{bias\_sweep\_rate}\}$  is the bias voltage sweep rate.
9. Go to step 3.